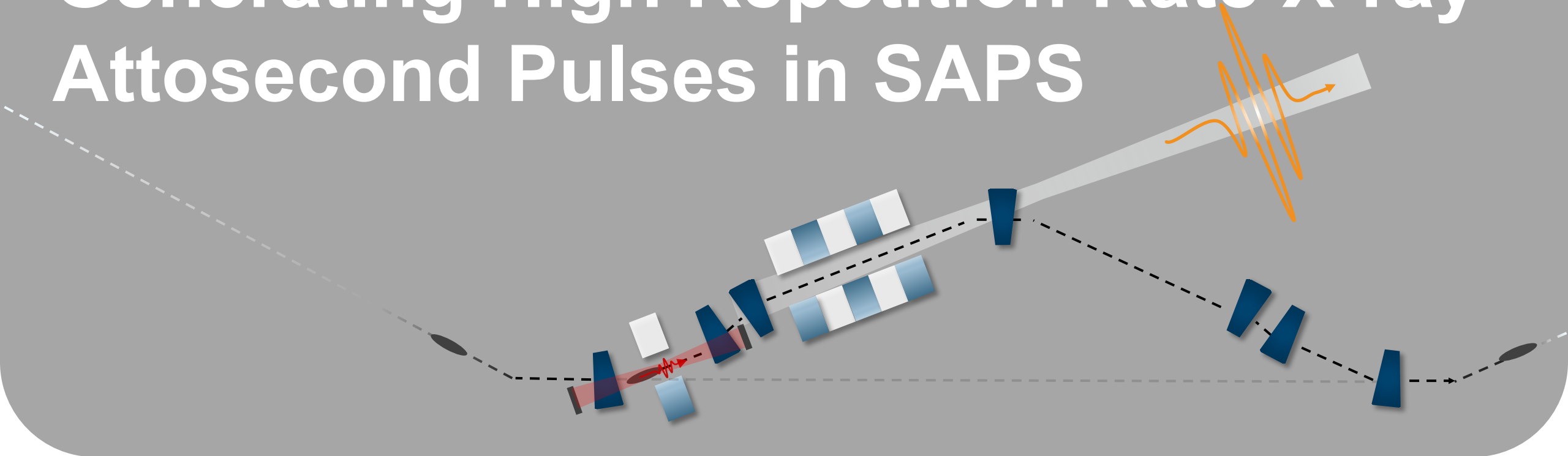


Generating High Repetition Rate X-ray Attosecond Pulses in SAPS



Weihang Liu

Future Light Sources 2023



Content

1. Introduction to SAPS
2. Background of attosecond pulse generation method
3. Method and performance
4. Improvement of repetition rate
5. Conclusion

Introduction to SAPS

SAPS, which stands for Southern Advanced Photon Source

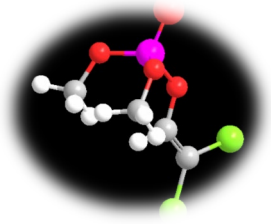


A fourth-generation diffraction-limited storage ring light source. It's planned to be built near the China Spallation Neutron Source in the southern region of China (CSNS). Design goal: Achieve high brightness ($> 1e22$).

	E(GeV)	C(m)	I (mA)	ϵ (pm)	Brightness	Damping Time
MAX-IV	3	528	500	326	3e21	25
Sirius	3	518	350	250	2e21	22
SLS-II	2.7	288	400	157	1e21	7.5
Diamond-II	3.5	560	300	157	3e21	19.5
NSLS-II_U	3	792	500	34.2	1e21	50
SAPS	3.5	810	500	< 60	> 1e22	<30

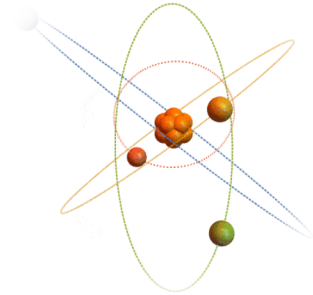
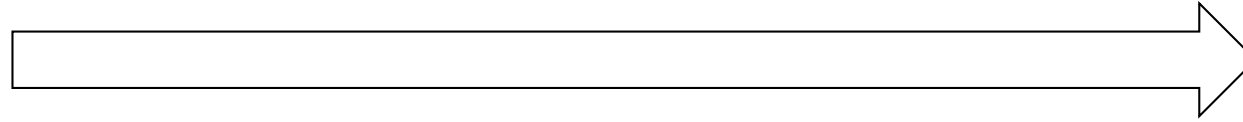
Research goal: to achieve a coherent attosecond beamline in SAPS with high repetition rate ($> 6\text{kHz}$) and high average flux ($> 10^9$ photons/s/(%bw))

Background Why Attosecond ?



molecular structural deformation processes

From femtosecond to attosecond



Real-time observation of electronic motion deep inside atoms

Possible applications

Observation the motion of Cooper pair electron

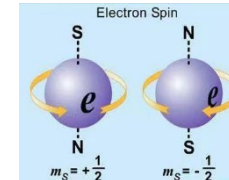
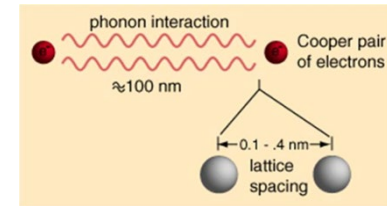
Understanding the high-temperature superconductivity

“See” the spin exchange process

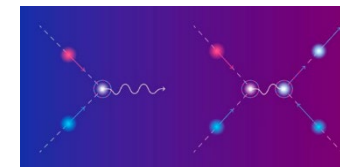
Study the Ultrafast Magnetization Dynamics

Observation of the electron-hole pair separation and recombination

Deep understanding the physical mechanism of PN junction

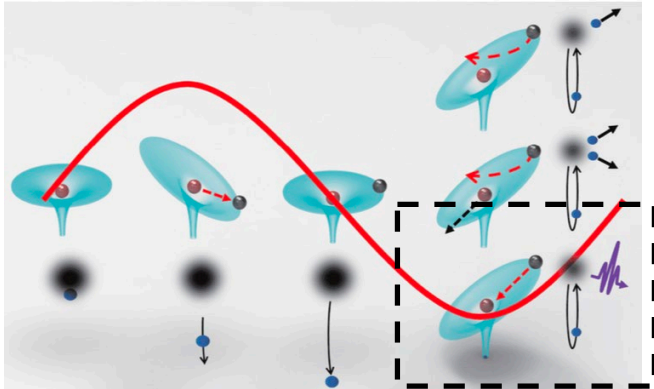


~100as



Background Attosecond pulse in HHG-based sources

high harmonic generation (HHG)

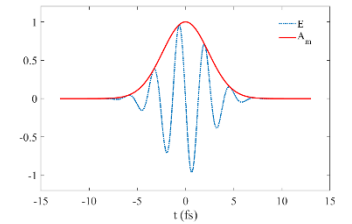


A strong, near-infrared laser was adopted to drive electrons in a gas, leading to harmonic up-conversion of the driving laser.

Attosecond pulse
Few-cycle laser
 High stability of CEP control guarantees good repeatability

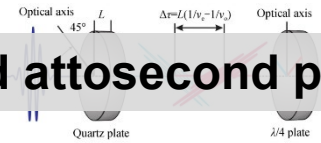
Gating

Amplitude gating



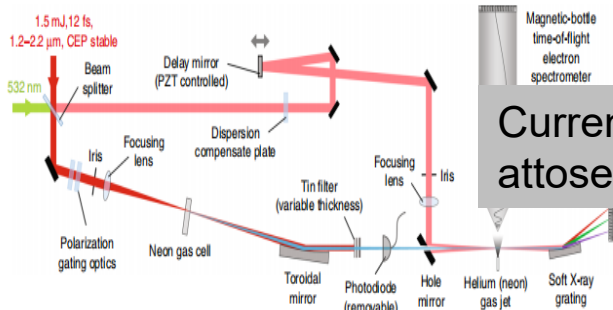
Polarization gating

Isolated attosecond pulses

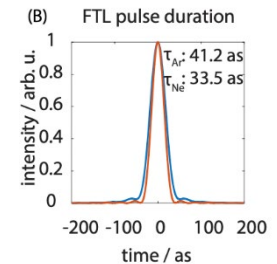
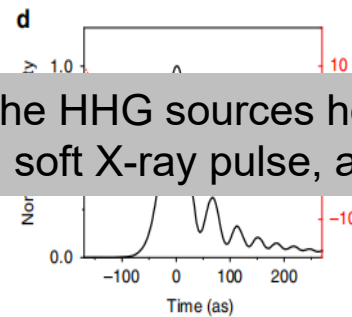


Double optical gating

Two color laser shaping the laser field



Currently, the HHG sources hold the record for the shortest attosecond soft X-ray pulse, at approximately 43 as



J. Li et al. Nature Communications, 8(1), aug 2017

T. Gaumnitz et al. Optics Express, 25(22):27506, oct 2017

Due to the low conversion efficiency, the photon flux is low (~10³ photons/pulse/1%bw)

Background Free electron laser (FEL)

Beam shaping:

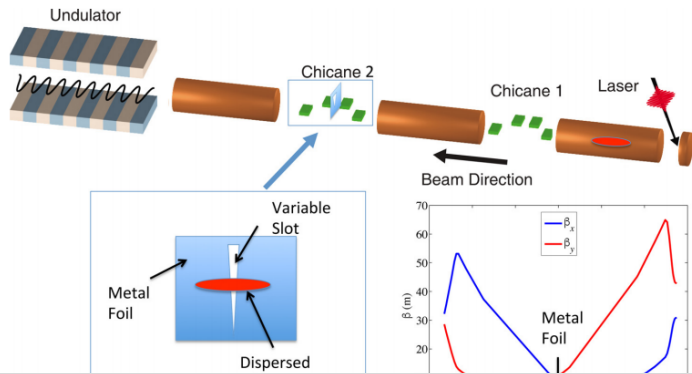


FIG. 1. Conceptual illustration of the scheme: the electron beam is accelerated and compressed in the LCLS linac. In the second chicane, a slotted metal foil spoils all but a short temporal spike of the electron beam. The bottom right plot shows the vertical and horizontal beta function in the second chicane.

duration ~ 400 as, wavelength \sim hard x-ray

Marinelli A, et al., Applied Physics Letters, 2017, 111(15): 151101.

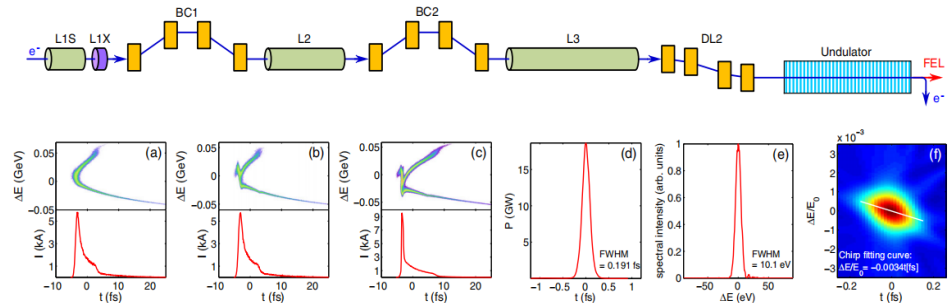


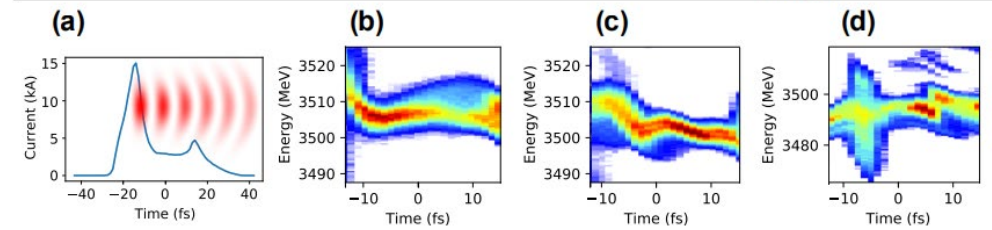
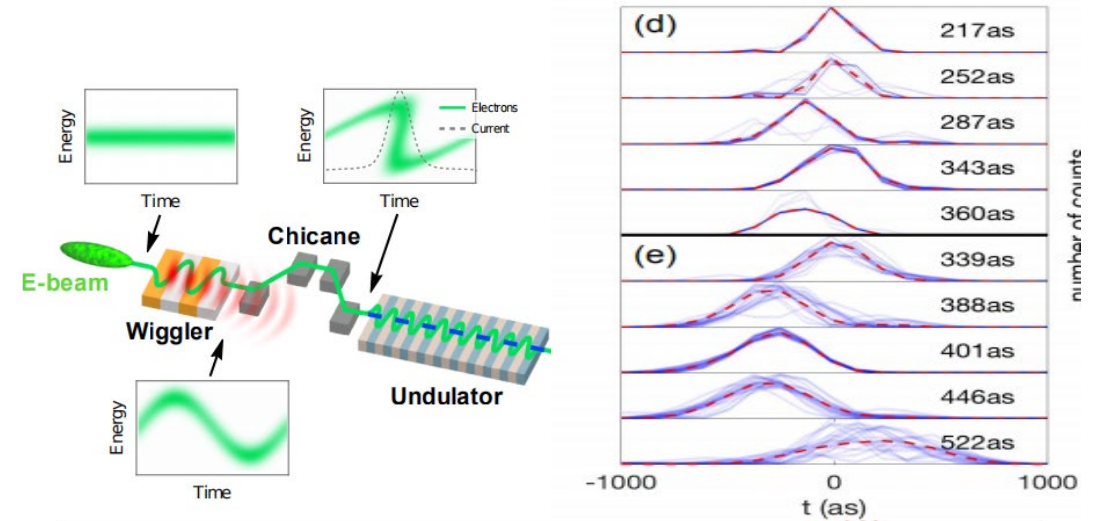
FIG. 1. A sketch of nonlinear bunch compression at the LCLS. At the top is a layout of the LCLS, with main lines S-band sections L1S and L1X, and the undulator. The bottom part shows the beam characteristics at different stages: (a) energy spread vs time, (b) energy spread vs time, (c) energy spread vs time, (d) power vs time, (e) spectral intensity vs energy spread, and (f) a 2D plot of energy spread vs time with a chip fitting curve. The FEL photon energy in this simulation is 5.6 keV. Bunch head is to the left.

duration ~ 179 as, wavelength \sim hard x-ray

The

Huang S, et al., Physical review letters, 2017, 119(15): 154801.

Beam shaping & Self-modulation enhanced SASE



Duris J, et al. Nature Photonics, 2020, 14(1): 30-36.

duration ~ 217 as, wavelength \sim soft x-ray

Background Free electron laser (FEL)

Beam shaping:

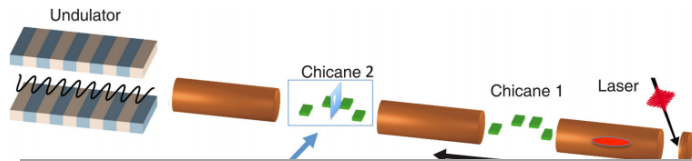
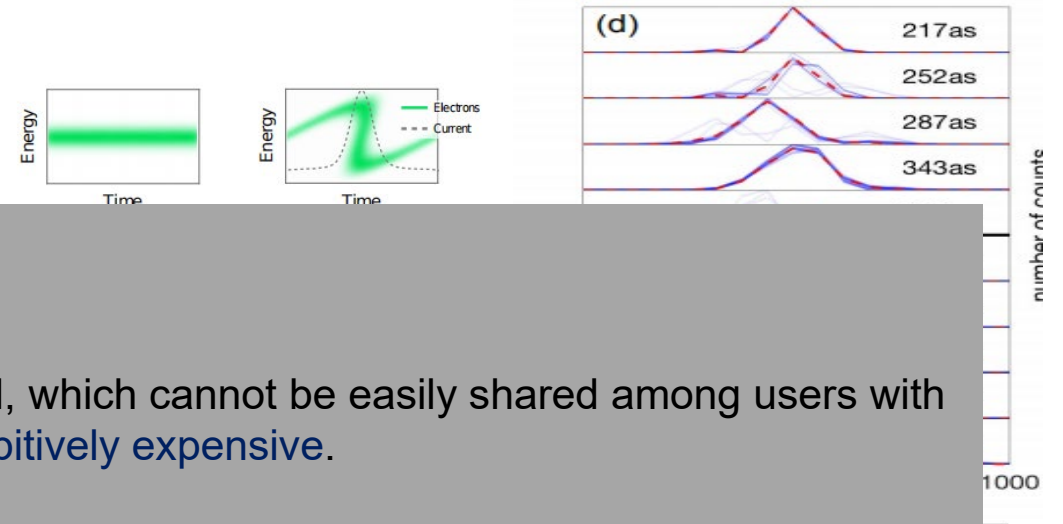


FIG. 1. Conceptual illustration of the

Beam shaping & Self-modulation enhanced SASE



Disadvantage:

those methods need to adopt the electron beam shaping method, which cannot be easily shared among users with different research needs, thus making the experiment time prohibitively expensive.

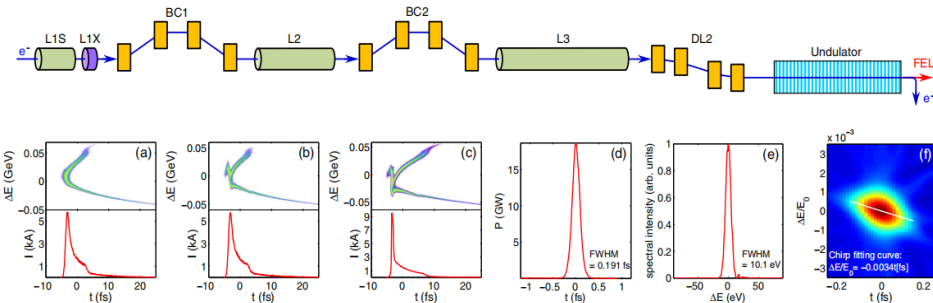
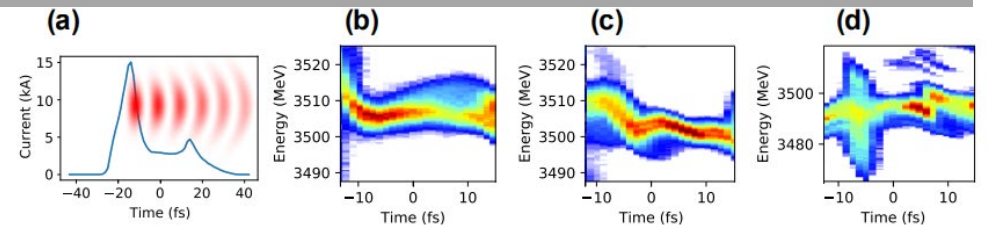


FIG. 1. A sketch of nonlinear bunch compression at the LCLS. At the top is a layout of the LCLS, with main lines S-band sections. duration ~ 179 as, wavelength \sim hard x-ray

The FEL photon energy in this simulation is 5.6 keV. Bunch head is to the left.

Huang S, et al., Physical review letters, 2017, 119(15): 154801.



Duris J, et al. Nature Photonics, 2020, 14(1): 30-36.

duration ~ 217 as, wavelength \sim soft x-ray

Background Advantages of storage rings

The storage ring-based light source is a stable, high repetition rate, a multi-user light source that has been at the forefront of high-brilliance experiments. It has evolved from the third generation to the fourth generation, also known as the diffraction-limited storage ring (DLSR), increasing brilliance by more than two orders of magnitude. Due to these advantages, the ability to achieve attosecond pulses in DLSRs would make them very attractive.

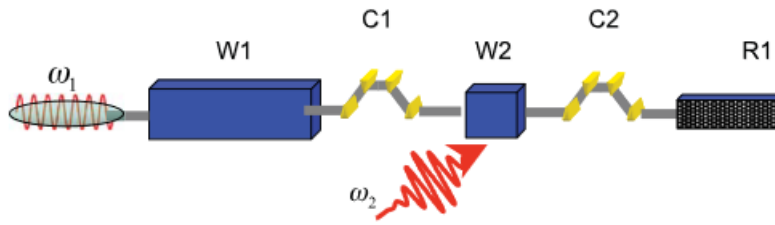
By achieving high-brilliance and providing high-flux and high repetition rate attosecond pulses, DLSRs can make great contributions to the development of attosecond science.

In DLSR, the natural light pulse is typically **in the range of 10 ps to 100 ps** due to the stretching of the electron beam length to reduce the collective effects. obtaining an attosecond pulse by **shortening the electron beam length** or by **slicing only a fraction of the electrons** for synchrotron radiation means a huge reduction in flux.

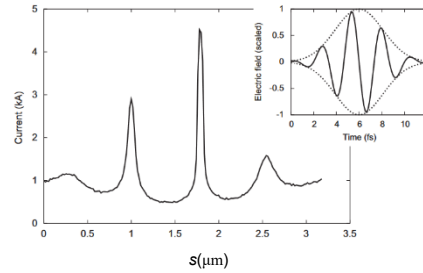
To achieve a **high-flux** attosecond pulse, need **coherent radiation**

attosecond pulse in storage ring EEHG

EEHG + few-cycle laser

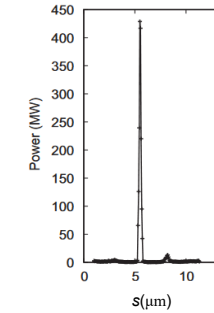
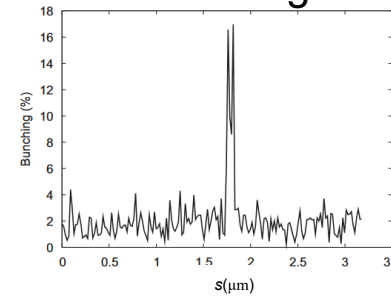


A. Zholents & G. Penn. NIM-A 612 (2010)



current amplifier

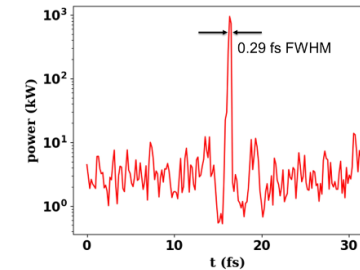
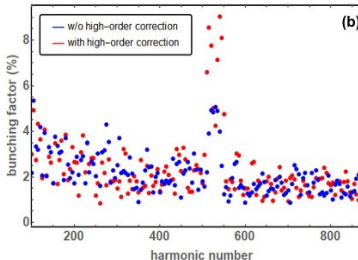
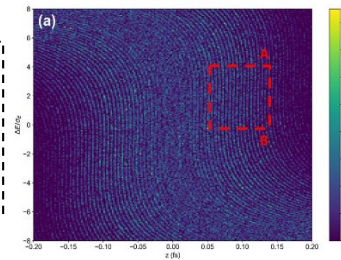
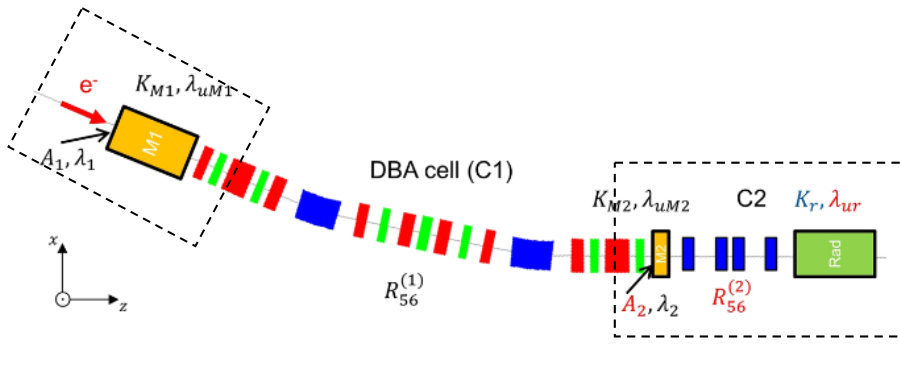
local bunching factor



260 as FWHM
102 nJ pulse

$$b_n(s) = \frac{\int_{s-\pi/k_L n}^{s+\pi/k_L n} I(\tau) / I_0 \exp(-ik_L n \tau) d\tau}{\int_{s-\pi/k_L n}^{s+\pi/k_L n} I(\tau) / I_0 d\tau}$$

Application to BESSY II Storage Ring



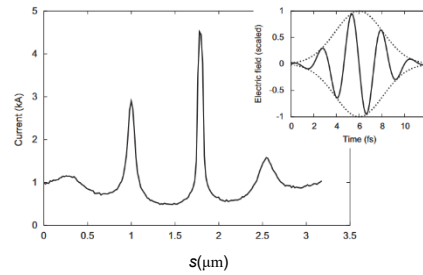
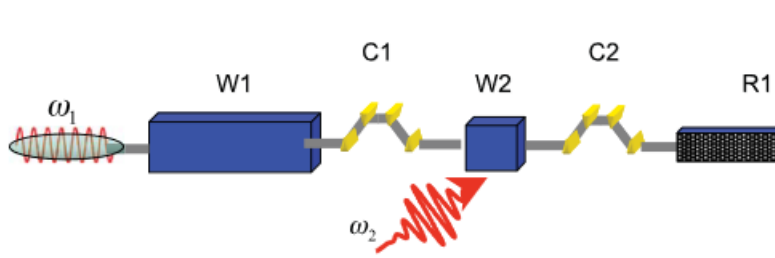
Repetition rate 6KHz
290 as FWHM
average flux $\sim 10^9$
phs/s/0.1% BW

Connecting two straight sections using an achromatic cell as the first chicane.

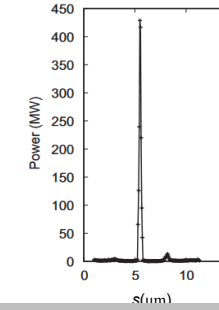
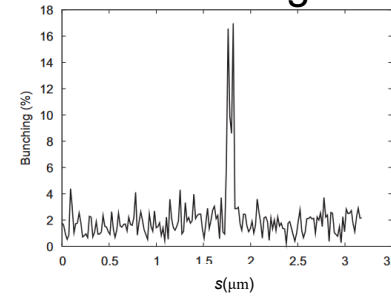
J.-G. Hwang, et al. Scientific Reports 10, 10093 (2020)

attosecond pulse in storage ring EEHG

EEHG + few-cycle laser



local bunching factor



260 as FWHM
102 nJ pulse

Drawbacks:

1. EEHG requires two lasers, and the second laser is a short-duration laser with few cycles, which makes it very difficult to synchronize the two lasers with the electron beam.
2. EEHG layout occupies two straight sections but supports only one experimental station.

J.-G. Hwang, et al. Scientific Reports 10, 10093 (2020)

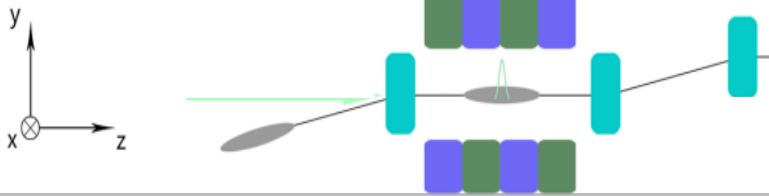
Content

1. Introduction to SAPS
2. Background of attosecond pulse generation method
- 3. Method and performance**
4. Improvement of repetition rate
5. Conclusion

Method ADM + few-cycle laser

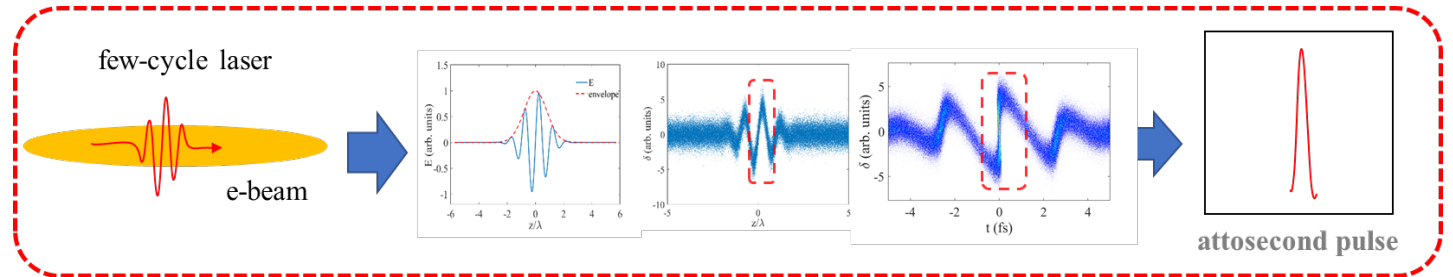
Angular dispersion-induced microbunching (ADM)

Feng Chao, and Zhentang Zhao. Scientific Reports 7 (2017).



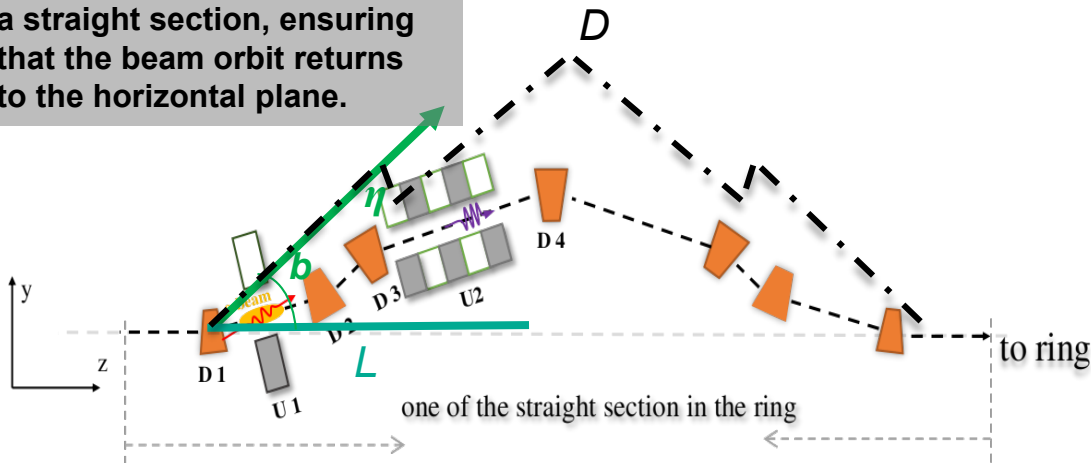
Using a weak dipole and dogleg to couple the electron transverse and longitudinal motions. Benefiting from low vertical emittance of the ring ADM can generate strong microbunching.

By a few-cycle laser, sub-fs individual microbunch can be generated



- $\sigma_b \geq 10$ ps, $\sigma_{\text{laser}} \sim 4$ fs, accommodate large time jitter. Easy synchronization.
- $\langle \varepsilon \rangle = \varepsilon_0 + \Delta\varepsilon \sim \varepsilon_0$, $\langle \sigma_\delta \rangle = \sigma_{\delta 0} + \Delta\sigma_\delta \sim \sigma_{\delta 0}$, the brilliance of other IDs is not affected.

All dipole elements are symmetrically distributed in a straight section, ensuring that the beam orbit returns to the horizontal plane.



ADM opt.cond.

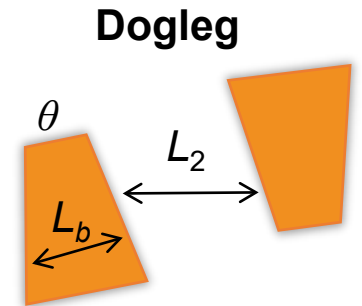
$$\begin{cases} r_{56} = -b\eta \\ 1 + hr_{56} = 0 \end{cases}$$

Dogleg par.cond.

$$\begin{cases} (L_2 + L_b)\theta = \eta \\ (L_2 + 2L_b/3)\theta^2 = r_{56} \end{cases}$$

$$(3L_b/2h)^{1/2} \leq \eta < (3L_{eff}/2h)^{1/2}$$

$$L_{eff} = (L - 2L_1 - 2L_3 - 5L_b)^2 / (3L - 6L_1 - 6L_3 - 17L_b)$$



Given the laser parameter (h), the only optimizable variable for ADM is dogleg dispersion η . and its value interval is restricted to the space of the straight section.

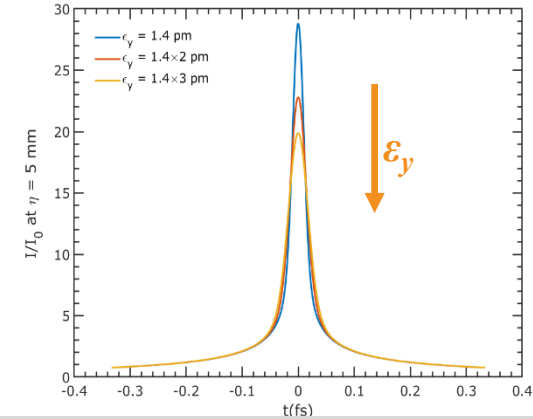
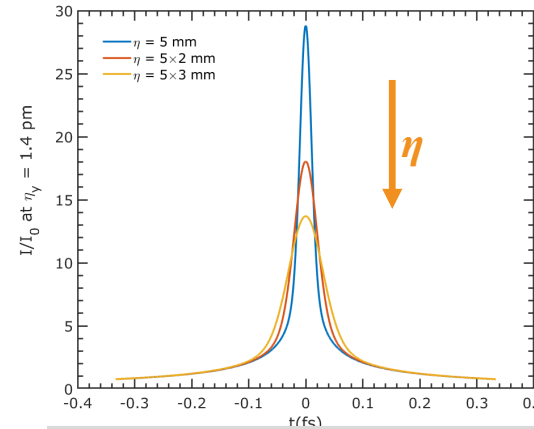
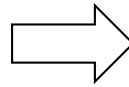
Parameters opt.

Optimization Objectives

After modulation, a current spike is generated in the electron beam:

$$I(s)/I_0 = 1 + 2 \sum_{m=1}^{\infty} f(m) \cos(k_L m s)$$

$$f(m) = \frac{0.67}{m^{1/3}} \exp\left[-\frac{1}{2} (m k_L \eta)^2 \gamma_y \epsilon_y\right]$$

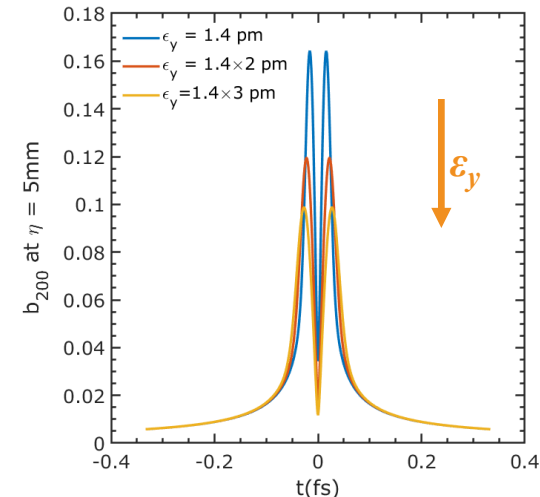
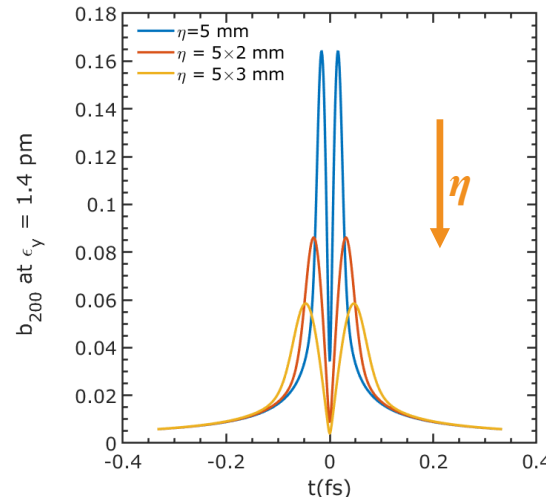
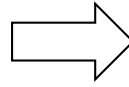


Local bunching factor:

$$b_n(s) = \frac{\int_{s-\pi/k_L n}^{s+\pi/k_L n} I(\tau)/I_0 \exp(-ik_L n \tau) d\tau}{\int_{s-\pi/k_L n}^{s+\pi/k_L n} I(\tau)/I_0 d\tau}$$



$$b_n(s) = \frac{2 \sum_{m=1}^{\infty} f(m) \sin(m\pi/n) \frac{m \cos(k_L m s) + i n \sin(k_L m s)}{n^2 - m^2}}{\pi/n + 2 \sum_{m=1}^{\infty} f(m) \sin(m\pi/n) \frac{\cos(k_L m s)}{m}} \exp(-ik_L n s)$$



more sensitive to dispersion compared to emittance.

In order to obtain high radiation power, a sufficiently large I/I_0 and local bunching factor are required. They all need **low** η and ϵ_y .

Parameters opt.

Optimizing the dogleg dispersion η :

$$\varepsilon_y = \varepsilon_y(\eta) + \kappa \varepsilon_x$$

Betatron Coupling

To obtain a small ε_y , it is necessary to control the betatron coupling to a small level, which we assume to be **0.4%** (0.4% ε_y from betatron coupling).

ε_y is a function of η

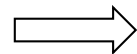
To take into account the **intra-beam scattering (IBS) effect**, we adopt the completely integrated modified Piwinski approximation method*:

$$\frac{d\varepsilon_x}{dt} = -\frac{2}{\tau_x}(\varepsilon_x - \varepsilon_{x0}) + \frac{2\varepsilon_x}{T_x(\varepsilon_x, \varepsilon_y, \sigma_\delta, \sigma_s)}$$

$$\frac{d\varepsilon_y}{dt} = -\frac{2}{\tau_y}(\varepsilon_y - \varepsilon_{y0}) + \frac{2\varepsilon_y}{T_y(\varepsilon_x, \varepsilon_y, \sigma_\delta, \sigma_s)}$$

$$\frac{d\sigma_\delta}{dt} = -\frac{2}{\tau_p}(\sigma_\delta - \sigma_{\delta0}) + \frac{2\sigma_\delta}{T_p(\varepsilon_x, \varepsilon_y, \sigma_\delta, \sigma_s)}$$

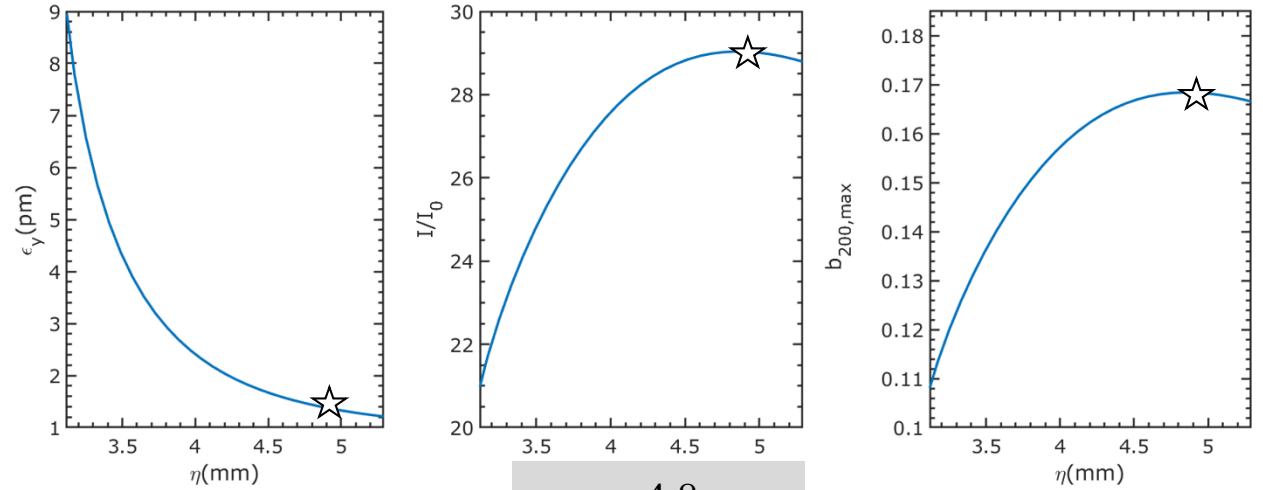
equilibrium



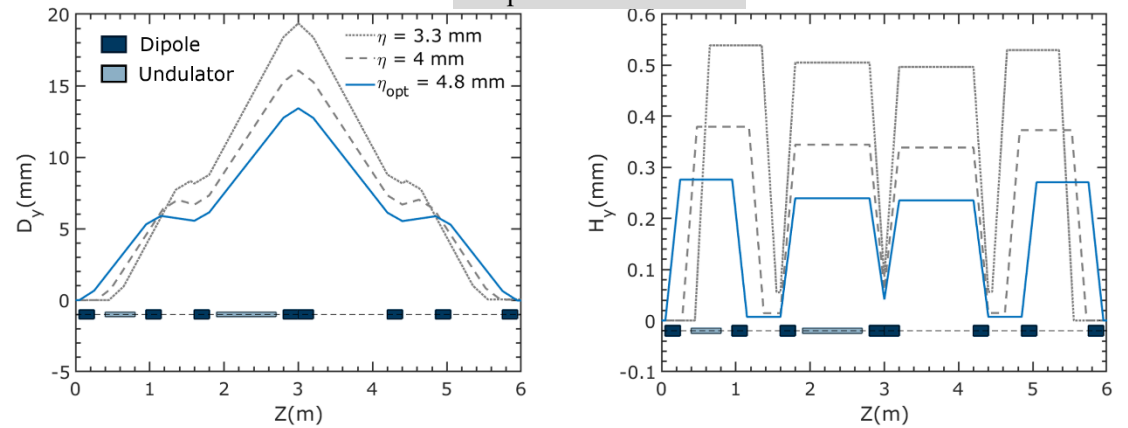
$$\varepsilon_x = \frac{\tau_x}{T_x} \varepsilon_x + \varepsilon_{x0}$$

$$\varepsilon_y = \frac{\tau_y}{T_y} \varepsilon_y + \varepsilon_{y0} \quad \varepsilon_y = \varepsilon_y + \kappa \varepsilon_x$$

$$\sigma_\delta = \frac{\tau_p}{T_p} \sigma_\delta + \sigma_{\delta0}$$



$\eta_{opt} = 4.8 \text{ mm}$



ELEGANT (incl. IBS) for opt. η , beam parameters:

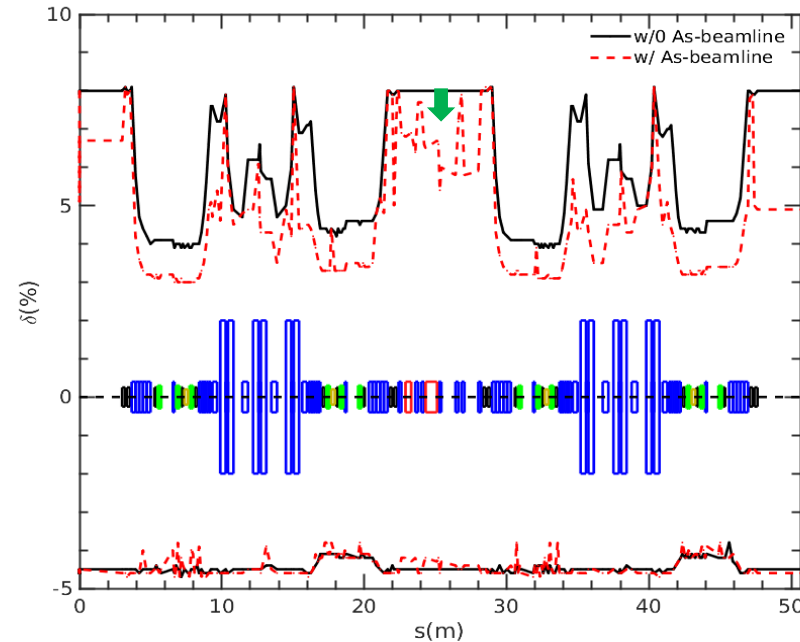
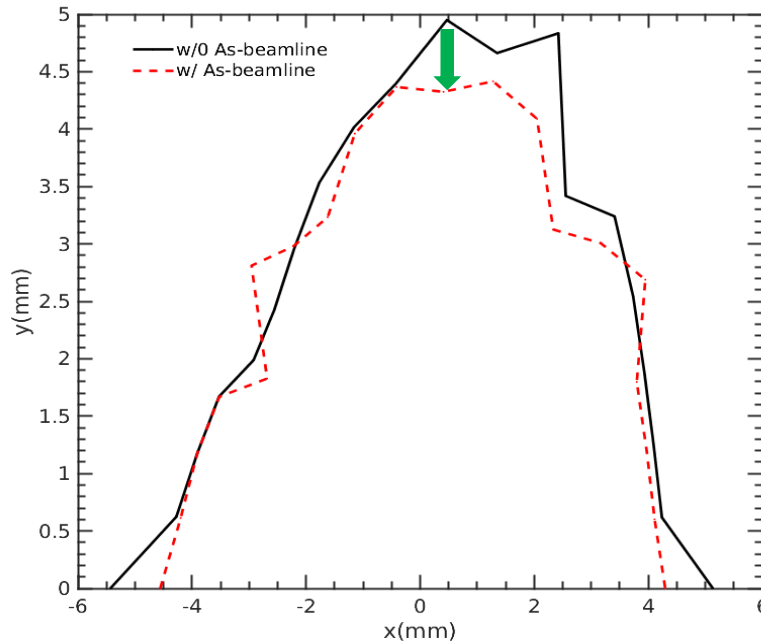
ε_x 100 pm, ε_y 1.4 pm, σ_δ 0.134%

Conforms well with the theoretical results.

Effect of ADM on storage ring dynamics

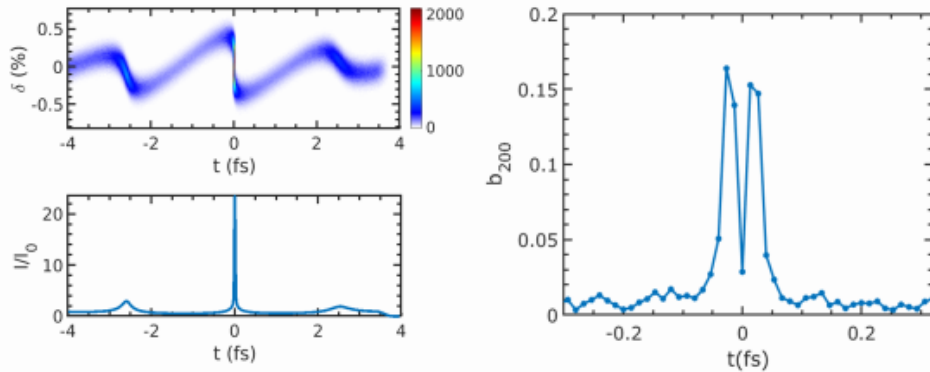
Reduction of DA and MA

the vertical dispersion introduced by the ADM section in the straight section breaks the periodicity of the storage ring and has some effects on the beam dynamics. The calculations show that both the dynamic aperture (DA) and the local momentum apertures (MA) are reduced. But, the DA reductions of less than 2% and the MA reductions of less than 25% have a negligible impact on the daily operation of the storage ring

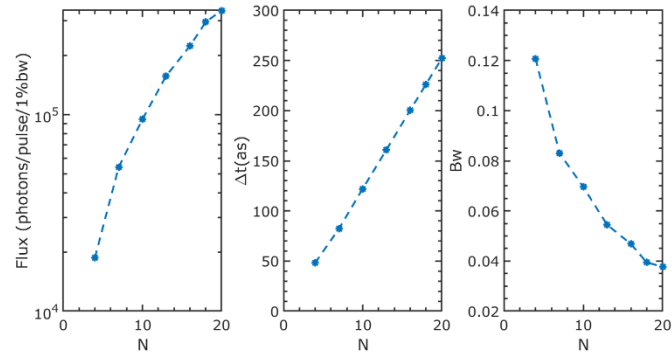


Performance

Modulation and radiation results

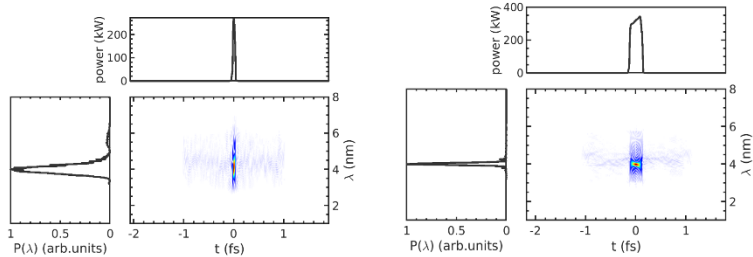


We adopted GENESIS and ELEGANT codes to perform simulation. Modulation results show local current is amplified by 24 times (v.s 19) and the peak local bunching factor is about 0.16 (v.s 0.17), which are in a great agreement with the theoretical optimal results.



Radiation results show Δt is directly proportional to N . The output radiation pulses are chirp-free attosecond pulses with time-bandwidth products are close to the Fourier transform limited ($\sim 1.83\text{fs}\cdot\text{eV}$).

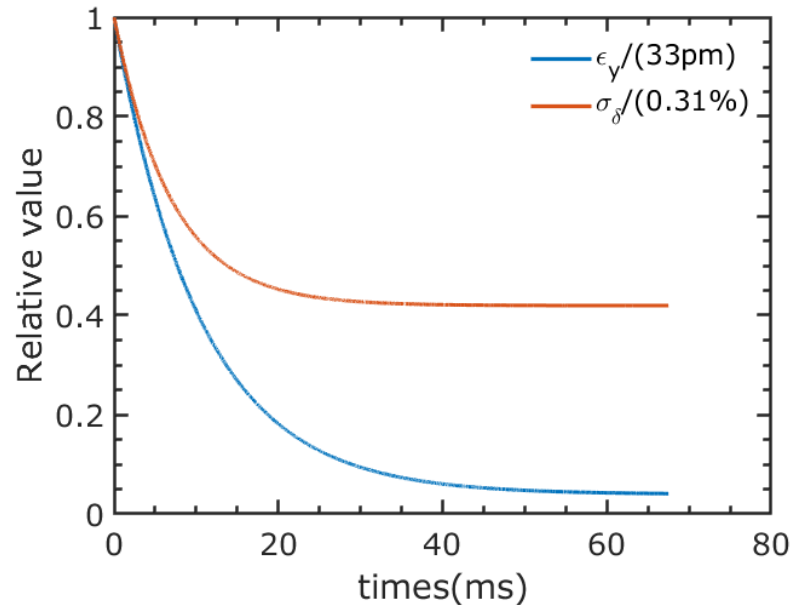
Period number	Δt (as)	Bw	Flux ($10^5\text{phs/pulse/1\%Bw}$)	$\Delta t\Delta E$ (fs·eV)
4	50	0.12	0.19	1.88
10	122	0.07	0.95	2.65
20	252	0.04	3.39	2.97



Performance

Repetition rate

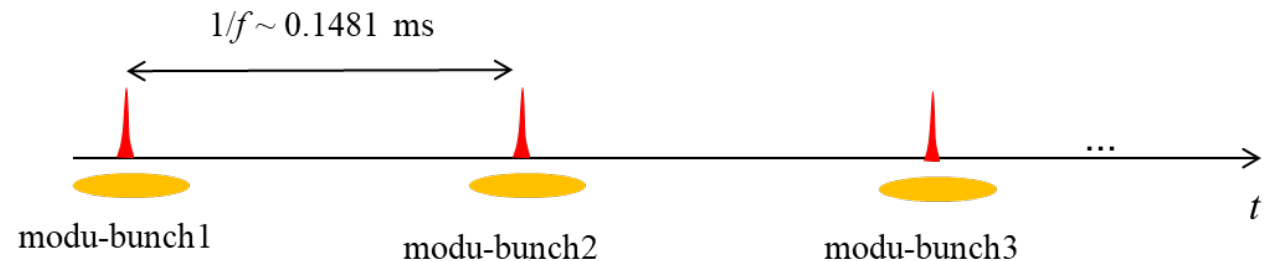
After modulation, vertical emittance and energy spread of this modulated portion increase. These parameters quickly return to their equilibrium values with the help of radiation damping. This happens within about four times the damping time, i.e., 60 ms.



modulated beam ϵ_y 3.4pm \rightarrow 33pm,
 σ_δ 0.134% \rightarrow 0.31%. return to their
equilibrium values after 60ms

Given the presence of 405 bunches in the ring, the repetition rate can reach up to **6.75 kHz**, provided that each bunch is modulated only once in each 60 ms recovery period.

Δt (as)	average flux (photons/s/(%bw))
50	0.128×10^9
122	0.64×10^9
252	2.29×10^9



Content

1. Introduction to SAPS
2. Background of attosecond pulse generation method
3. Method and performance
- 4. Improvement of repetition rate**
5. Conclusion

Improvement of repetition rate

laser delay and multiple modulations

It is worth noting that during each modulation, only a small part of the beam (with beam length σ_b) is modulated by the few-cycle laser (with duration σ_l). If multiple modulations of different parts of the bunch are carried out during each recovery period (60 ms), the repetition rate can be increased to a maximum of approximately σ_b/σ_l times.

However, after each modulation, the particles undergo a transverse betatron oscillation and are affected by the momentum compaction effect so that the modulated particles have a path length variation after one revolution. The equivalent path length difference of the modulated electron beam can be estimated as*

$$\sigma_L = \sqrt{(\alpha_p C \sigma_\delta)^2 + (\pi \xi_x \varepsilon_x + \pi \xi_y \varepsilon_y)^2}$$

where α_p is the momentum compaction factor, C is the circumference of the ring, $\xi_{x,y}$ are the chromaticities of the ring, σ_δ and $\varepsilon_{x,y}$ are energy spread and emittances of the modulated beam. The estimated value of σ_L is about 63 μm .

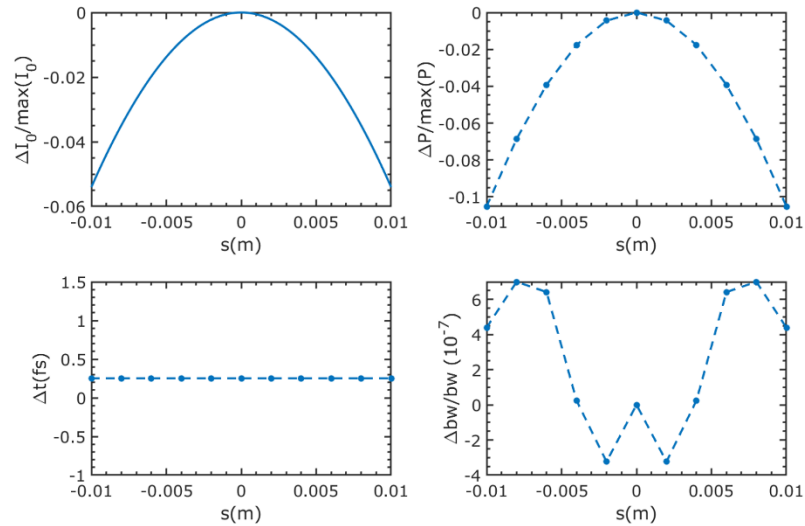
Furthermore, it is important to consider the Gaussian longitudinal distribution of the beam, as a delay distance that is too large can result in a decrease in local current.

*Shoji, Y. Phys. Rev. ST Accel. Beams 8, 094001 (2005)

Improvement of repetition rate

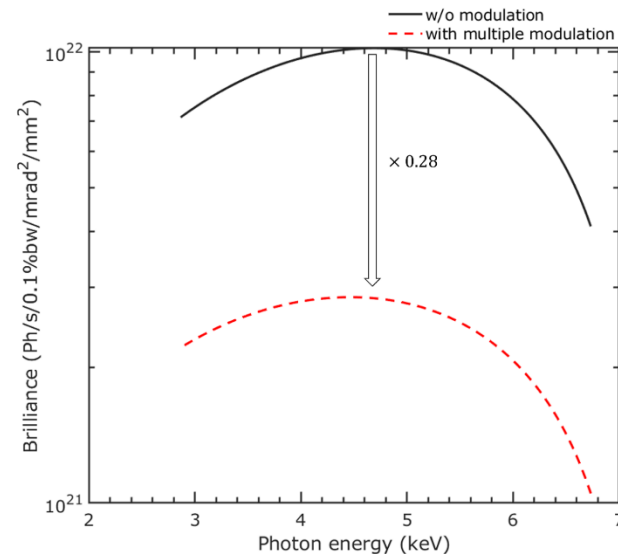
Repetition rate, performance and brightness

When a delay length of **0.1 mm** is selected and **200 modulations** are performed on the beam, the corresponding reduction in local current is maximally 6%, and there is a decrease in radiation power of approximately 10%. This suggests that multiple modulations generate radiation pulses with a variation magnitude of less than 10%. In this way, the repetition rate can be increased to 1.35 MHz.



Δt (as)	average flux (photons/s/(%bw))
50	0.247×10^{11}
122	1.23×10^{11}
252	4.4×10^{11}

In addition, the degradation of the beam parameters of the modulated beam after multiple modulations is more severe than that after a single modulation. This degradation significantly affects the brilliance of other IDs.



$\varepsilon_y \sim 33\text{pm}$, $\sigma_\delta \sim 0.31\%$
 The highest brilliance of an ID decreased by approximately 72%.

Content

1. Introduction to Southern Advanced Photon Source (SAPS)
2. Research Background
3. Program Design
4. Radiation Performance in Different Modes
5. Further Enhancement of Repetition Frequency
- 6. Discussion and conclusion**

Discussion and conclusion

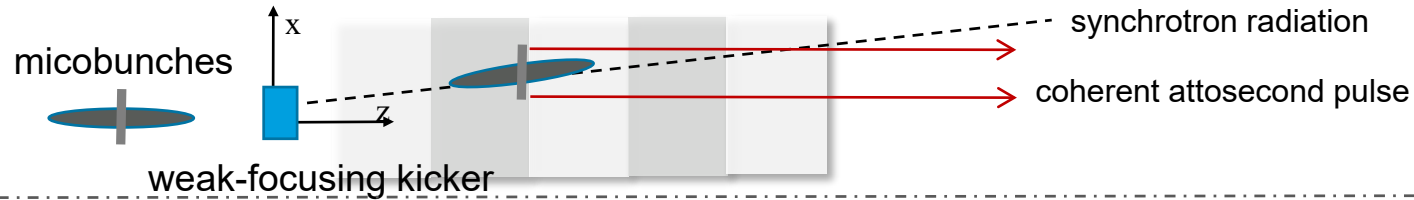
We proposed a method to generate attosecond pulses in SAPS by combining ADM and few cycle laser. simulations show attosecond pulse with repetition rate of 6.75kHz can be generated. By introducing a suitable time delay between the laser and the beam, the modulation can be performed repeatedly on a beam, thereby increasing the repetition rate to 1.35MHz.

Ongoing and future works:

1. pulse duration variation with period number variable undulator (using segmented undulators and adjusting the gap to control the number of periods, phase shift issue?)
2. Improve signal-to-noise ratio
 - increase current? Not favored by storage ring dynamics
 - Separation of the attosecond pulse [next slide]
3. Design a laser delay system for high repetition rate mode

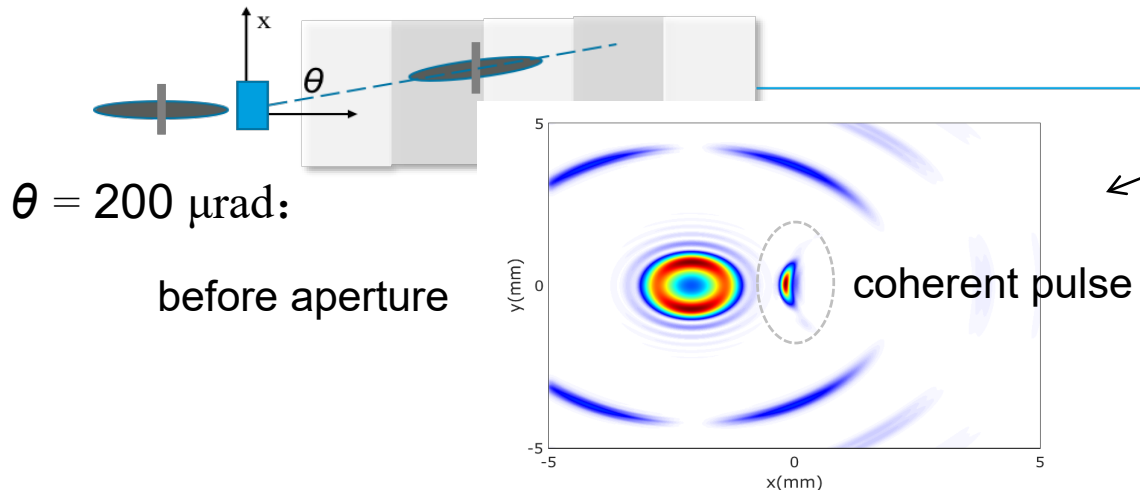
separation of the attosecond pulse Not yet completed

Idea Beam dynamics and some FEL experiments have shown that, microbunches rotate toward the new direction of travel if the electron beam is kicked and defocused. This can be used for multiplexing at FEL. While under weak focusing kicker, the direction of microbunches is unchanged*.



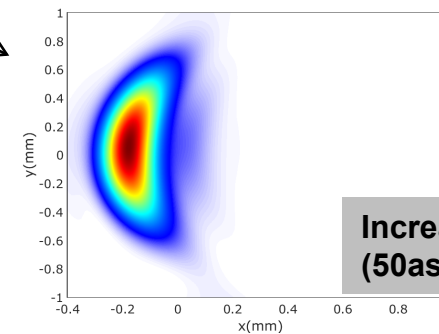
When the kick angle is large enough, we may isolate the attosecond pulse

Simulaton (code SRW)



10 m | Aperture:
x [-0.4mm, 1 mm]
y [-1 mm, 1 mm]

At a distance of 10 m from the source, we added a suitable aperture to separate the coherent radiation from the synchrotron radiation

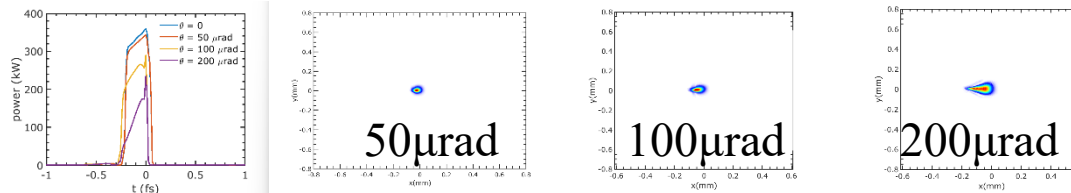


After aperture,
~99% attosecond pulse pass through
~0.1%, synchrotron radiation remainder

Increase the signal-to-noise ratio to 10~100 (50as ~ 252 as)

issues

As the increase in θ brings about a decrease in radiated power and coherence



A full optic beamline design is needed to see if those degradations are acceptable for the experimental requirements.

Thanks for listening

